Oral presentation | Numerical methods
Numerical methods-VII
Thu. Jul 18, 2024 2:00 PM - 4:00 PM Room A

[11-A-01] A small cell correction technique for multilevel Cartesian mesh methods

*Matthias Meinke[1], Tim Wegmann[1], Wolfgang Schröder[1] (1. Institute of Aerodynamics, RWTH Aachen University)

Keywords: Cartesian Mesh, Multilevel, Small cell

ICCFD 12, Kobe, July 14-19, 2024

A Small Cell Correction Technique for Multilevel Cartesian Mesh Methods

Matthias Meinke
T. Wegmann, F. Wietbüscher, W. Schröder
m.meinke@aia.rwth-aachen.de

Institute of Aerodynamics
RWTH Aachen University
Aachen, Germany

Outline

- Multiphysics Solver Framework m-AIA
- Cartesian Mesh Method
- Motivation for Multigrid
- Small Cell Correction
- Results for Steady Solutions
  - Flow around a Solid Body
  - Heat Conduction in Steel Casting
- Summary & Conclusions

Multiphysics Code: m-AIA

Main characteristics of the **multiphysics simulation framework m-AIA** developed at the Institute of Aerodynamics (> 200 man years invested)

- in-house code entirely written in C++ of the Institute of Aerodynamics, RWTH Aachen University
- main target: CFD, aeroacoustics, heat transfer, and structural mechanics, ≈ 400.000 code lines

CFD (Fluid Mechanics):

- **Finite-Volume method** for the Navier-Stokes equations based on block-structured and Cartesian meshes
- **Lattice Boltzmann method** based on Cartesian meshes

CAA (Aeroacoustics):

- **Discontinous Galerkin method** for the acoustic perturbation equations on Cartesian meshes

Structural Mechanics:

- **Finite Cell method** based on Cartesian meshes

Heat Conduction:

- **Finite Volume method** for the heat conduction equation on Cartesian meshes

Lagrangian Particle Tracking:

- Tracking of point particles, e.g. for **spray modelling** or the **transport of particles**

Coupling of Multiphysics Solvers in m-AIA

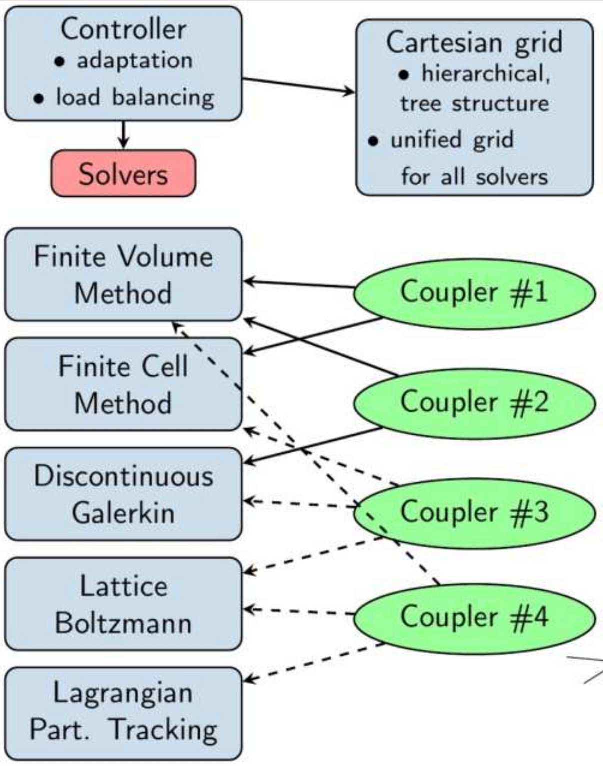

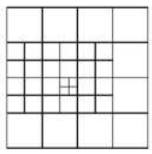

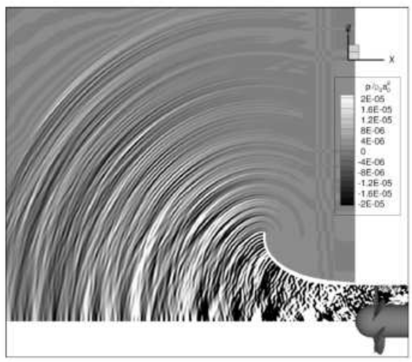

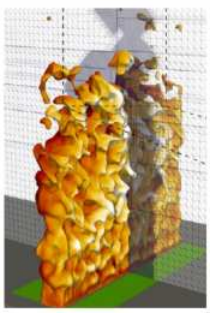

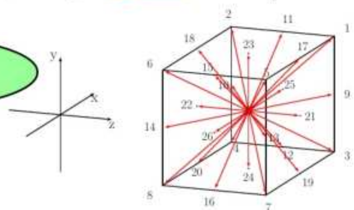

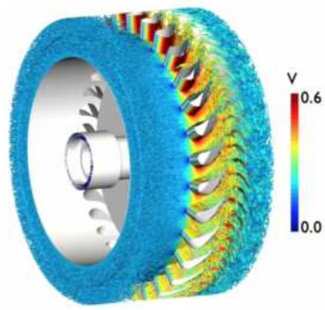

Landing Gear Noise (EU-Project Inventor)

LAGOON nose landing gear with additional components

- Simplified nose landing gear to study systematically NRT
- Investigated numerically and experimentally
- $Re_D = 350,000$, $M = 0.1$ (wind tunnel)

Porous fairing

- Fairings with different kind of porous materials , e.g., cluster of multiple units of the diamond lattice cell
- Objective to mitigate broadband noise generated by vortex-surface interactions

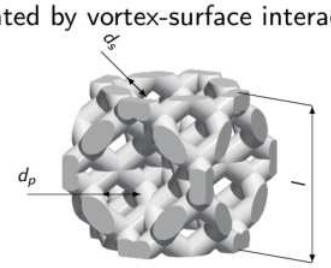

Diamond lattice structure, $l = 2.5mm$

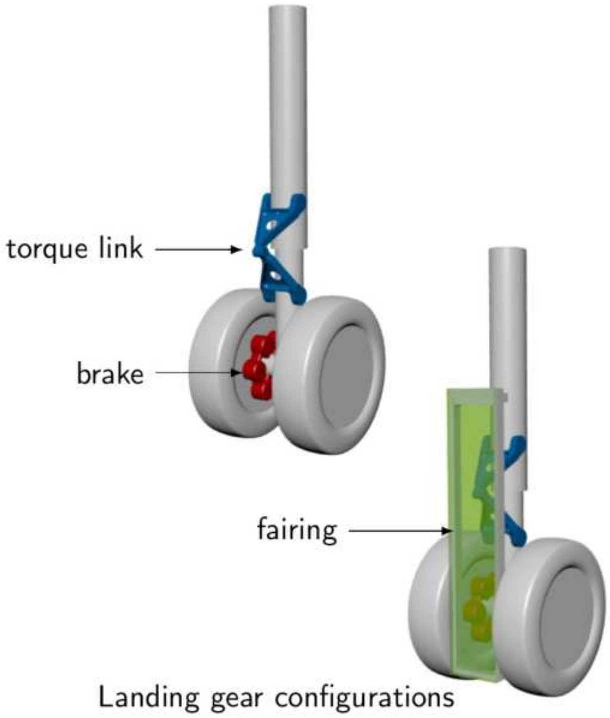

Landing gear configurations

Landing Gear: Numerical Setup

CFD: Lattice Boltzmann Method

- Collision step based on countable cumulants
- Sponge layer using artificial viscosity
- CBC by solving the LODI equations

Computational domain

- Domain size: (130 x 65 x 32.5) D
- Physical domain size: (80 x 40 x 20) D

Grid	noCells/D	dt [s]	noCells
coarse	252	1e-06	150 million
medium	504	5e-07	200 million
fine	1008	2.5e-07	705 million

CAA: Ffowcs Williams and Hawkings method

- Solved in frequency or time domain
- $\approx 1.8 \cdot 10^{10}$ data points in space-time

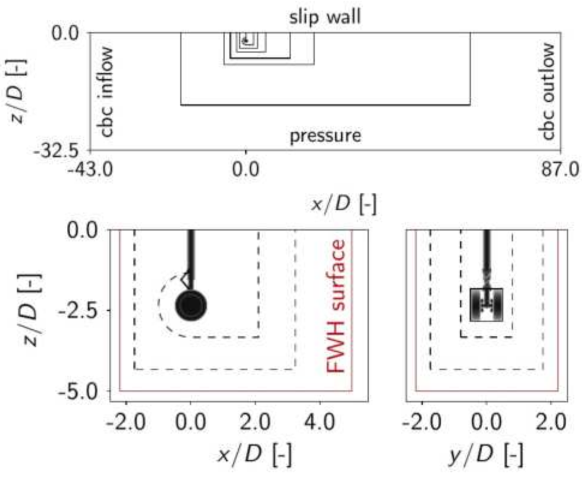

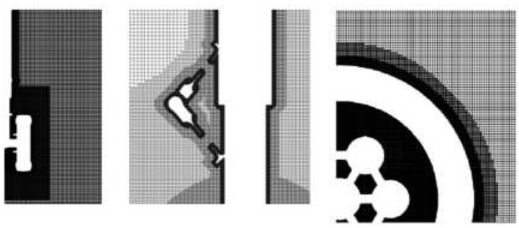

Landing Gear: Flow Field Results

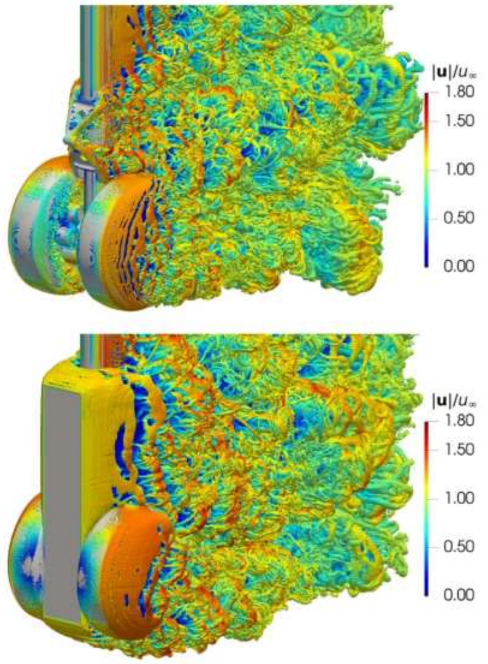

RWTH Cumulant LBM solution:
Instantaneous velocity on Q-criterion

Comparisons with other solvers

- CHALMERS: Star-CCM +
- ONERA: ZDES (RANS/LES)
- RWTH: m-AIA, cumulant LBM
- TUD: PowerFLOW, LBM

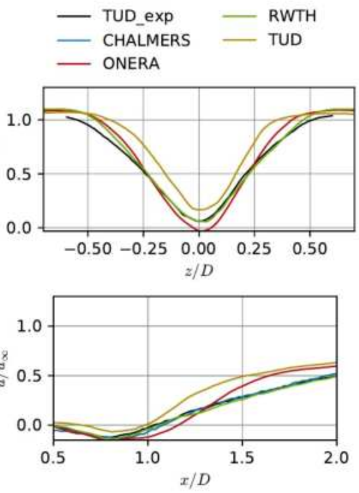

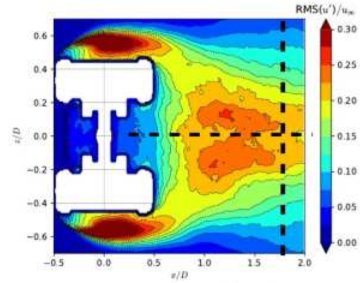

Location of probe lines

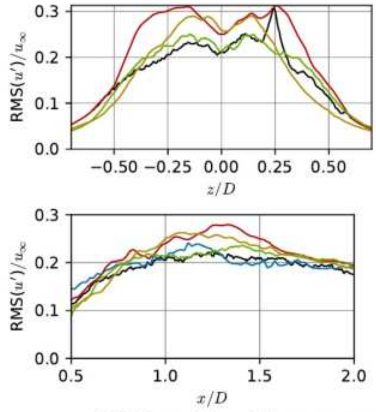

Propeller Noise (EU Project Enodise)

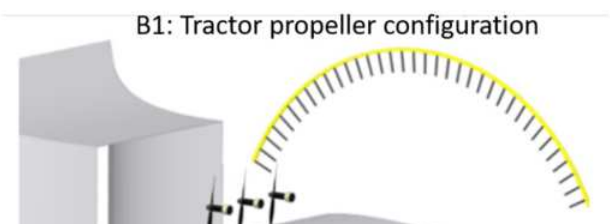

Objectives:

- Apply numerical methods and perform high-fidelity CFD/CAA simulations of propeller-wing/pylon setups
- Experiments performed in acoustic wind tunnels of project partners, e.g. TU Delft
- Investigate the noise mitigation effects, e.g. by leading-edge porous treatments

isolated propeller

installed propeller

Propeller Noise: Numerical Setup

CFD Method: Finite-Volume Solver

- Level-Set is used to track rotating surfaces
- adaptive mesh refinement to track the rotating propeller blades
- dynymic load balancing to maintain high parallel efficiency
- computational mesh size: 1400 million cells
- minimum spatial resolution at the solid surface: 0.07mm

Sketch of the computational domain

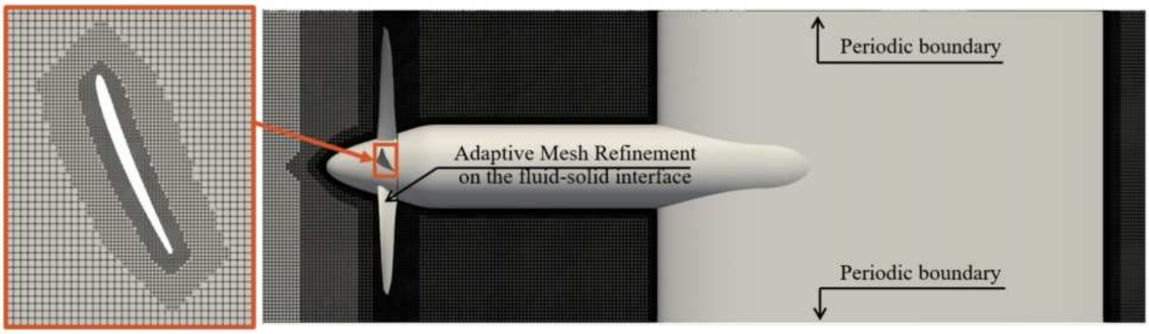

Propeller Noise: Simulation Results

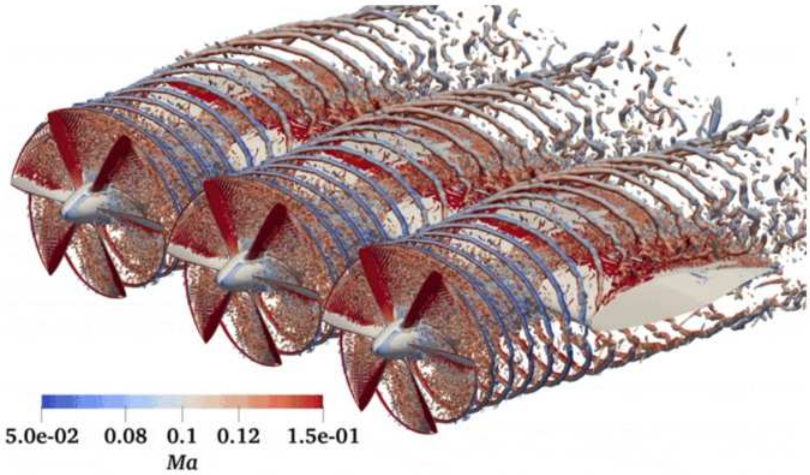

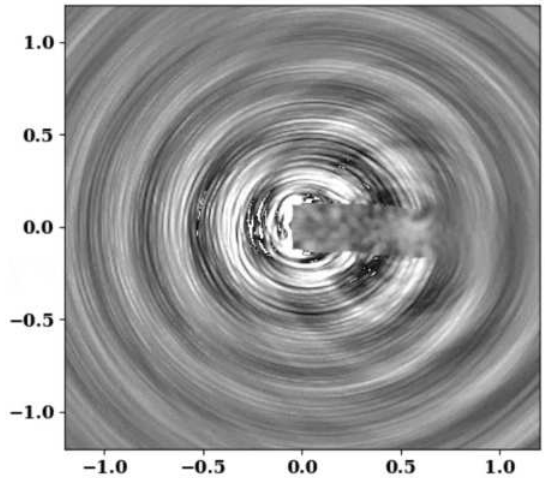

Visualization of the vortex structures (left) and the acoustic field (right)

Finite-Volume Solver for Cartesian Hierarchical Meshes

- Unstructured hierarchical Cartesian mesh and immersed boundary method
- Automatic parallel mesh generation[1]
- Adaptive mesh refinement and dynamic load balancing
- Multi cut-cell approach is applied to account for sharply resolved boundary surfaces
- **Small cell treatment by interpolation of variables and flux-redistribution to maintain conservation**
- Relative movement of objects without sliding mesh approach

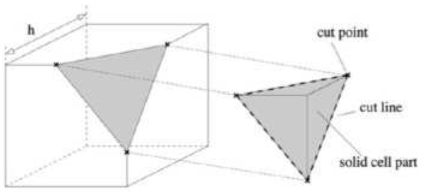

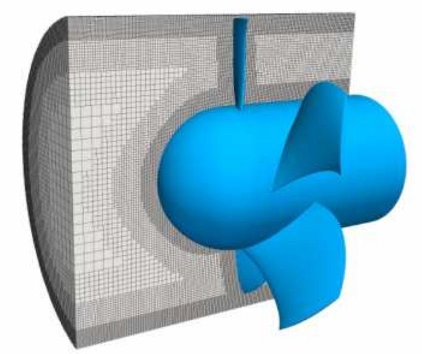

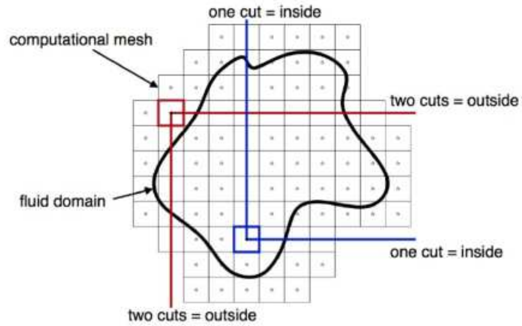

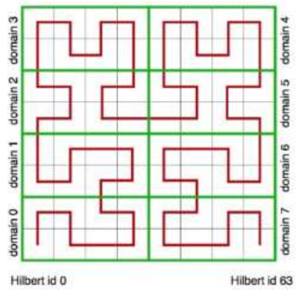

[1] Lintermann et al., Massively parallel grid generation on HPC systems, Comput. Meth. Appl. Mech. Eng., 2014

Cut-Cell Generation

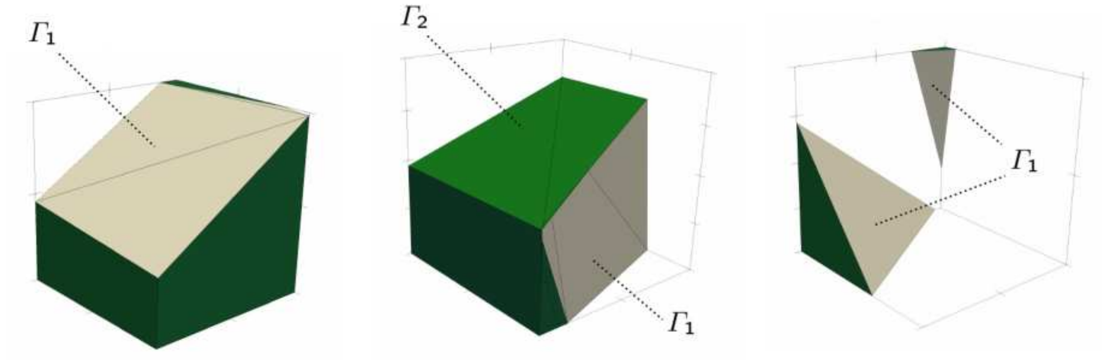

single cut cell multi cut cell split cell

- identify cut cell candidates using level-set values or STL data, determine cut point on the cell edges
- triangulation by marching cube algorithm, create polygonal cell representation for all cell intersections
- compute intersection of the individual polygons based on boolean set operations for binary space partitioning trees
- simplification of polygonal surface representation to reduce storage requirements for many internal interfaces.
- perform split cell treatment for cells with separate fluid volumes

Motivation: Particulate Flow

- Non-spherical shape of biomass particles results in a different interaction between the particles and flow structures
- Improved point particle models are required for non-spherical particles with an equivalent spherical diameter ≈ Kolmogorov length scale
- Particle resolved Direct Numerical Simulations can provide the required data for the derivation of such point-particle models

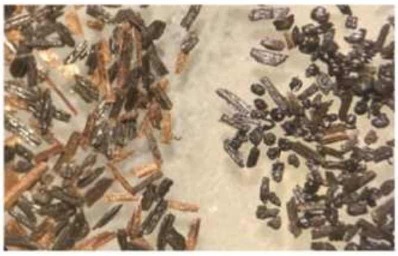

Miscanthus particles
(Panahi et al., 2017)

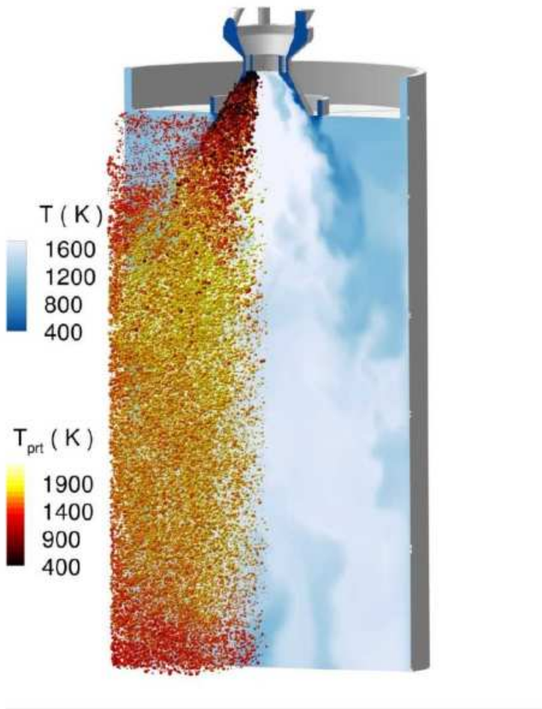

Force & Nusselt Number Correlations for Ellipsoidal Particles

- Correlations for drag, lift, and torque determined from **4400** single particle simulations
- Parameter space:
  - Particle Reynolds numbers: $1 \leq Re_p \leq 100$
  - Aspect ratios: $1 \leq \beta \leq 8$
  - Inclination angle: $0^\circ \leq \phi \leq 90^\circ$
- **Drag force:**
  $\hat{F}_D = \frac{1}{8}\rho\pi d_{eq}^2 |\hat{u}_f - \hat{u}_p|^2 C_{D,\phi}(Re_p, \beta)\hat{d}_D$
- Nusselt number correlations determined from **6600** single particle simulations

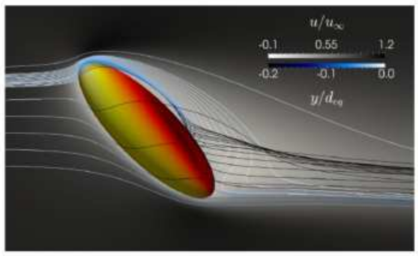

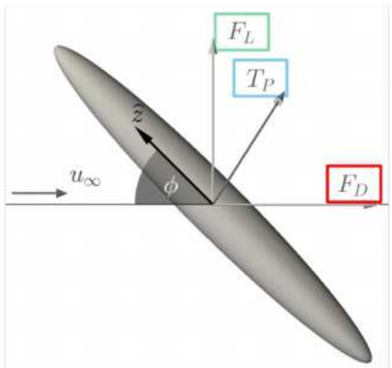

Fröhlich et al., *Correlations for inclined prolates based on highly resolved simulations*, JFM, 2020
Kiwitt et al., *Nusselt correlation for ellipsoidal particles*, IJMF, 2022

Force & Nusselt Number Correlations for Ellipsoidal Particles

- Correlations for drag, lift, and torque determined from **4400** single particle simulations
- Parameter space:
  - Particle Reynolds numbers: $1 \leq Re_p \leq 100$
  - Aspect ratios: $1 \leq \beta \leq 8$
  - Inclination angle: $0^\circ \leq \phi \leq 90^\circ$
- **Drag force:**
  $\hat{F}_D = \frac{1}{8}\rho\pi d_{eq}^2 |\hat{u}_f - \hat{u}_p|^2 C_{D,\phi}(Re_p, \beta)\hat{d}_D$
- Nusselt number correlations determined from **6600** single particle simulations

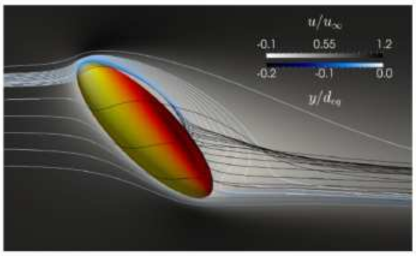

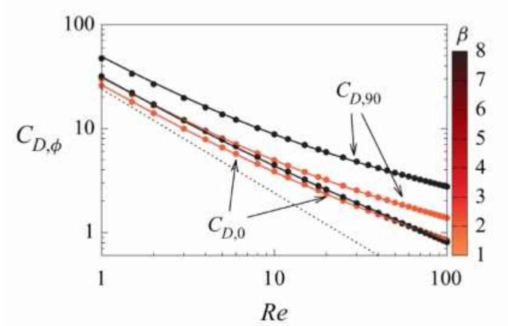

Fröhlich et al., *Correlations for inclined prolates based on highly resolved simulations*, JFM, 2020
Kiwitt et al., *Nusselt correlation for ellipsoidal particles*, IJMF, 2022

Motivation: Continuous Steel Casting (SMS Group GmbH)

http://www.stahlseite.de

Motivation: Continuous Steel Casting (SMS Group GmbH)

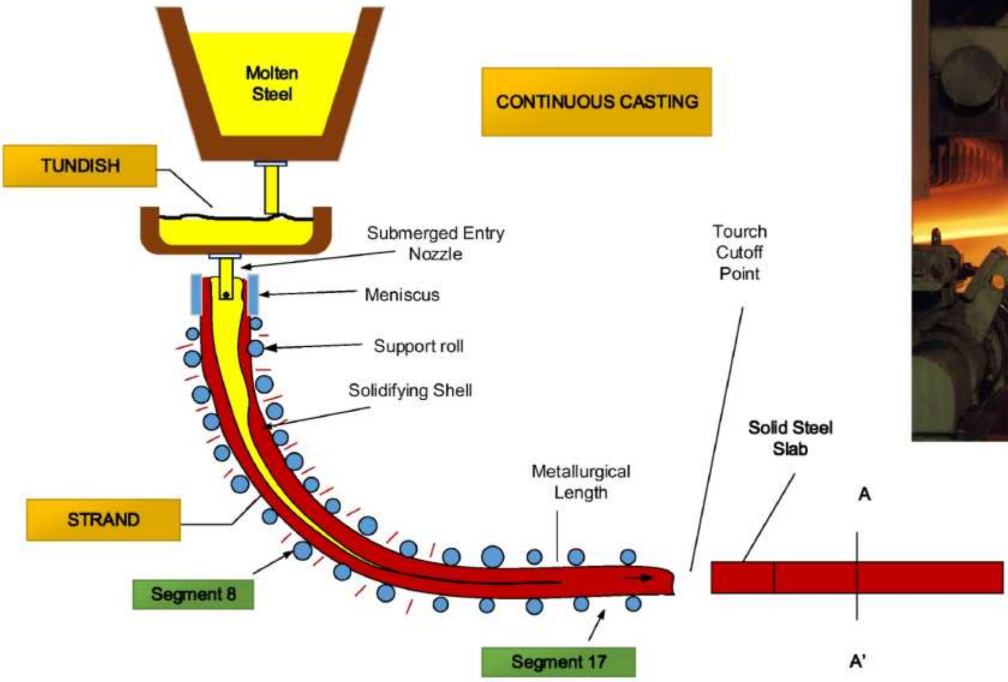

Steel Casting: Simulation Results

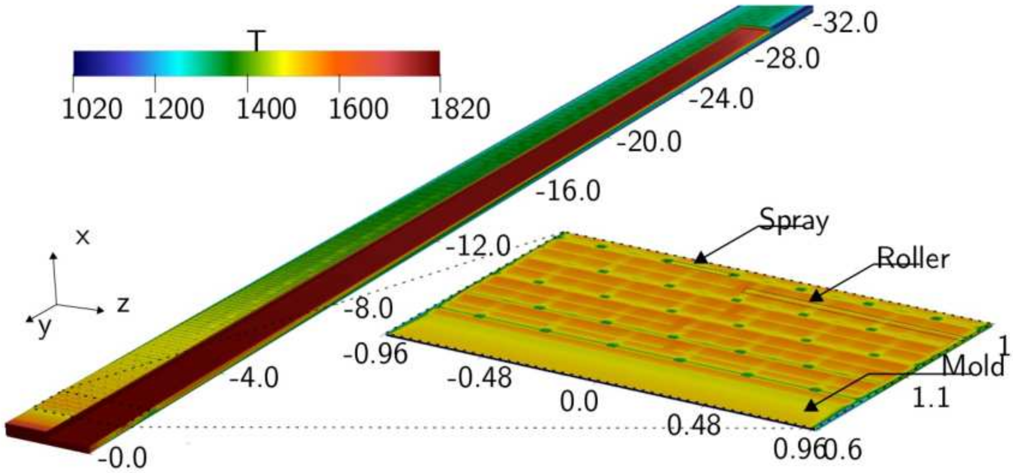

surface and core temperature distribution in the slab

Simulation of the temperature field in a slab

- Slab dimensions: 0.256 m x 1.92 m x 32.8 m
  O(50) million mesh cells, 4096 cores, O(1h) computing time
- more than 1000 patches for the different boundary conditions on the surface, i.e., radiation, roller contact, water spray

Steel Casting: Simulation Requirements

Caster design requires a large number of accurate temperature predictions

- variation of design parameters such as roller locations, steel alloys, spray configuration, slab dimensions
- temperature predictions are required for steady casting processes
- $\rightarrow$ acceleration to convergence by a multigrid method
- use several solver objects on increasingly coarser mesh levels
- coupler between the mesh levels is used for the determination of the defect correction and FAS interpolation

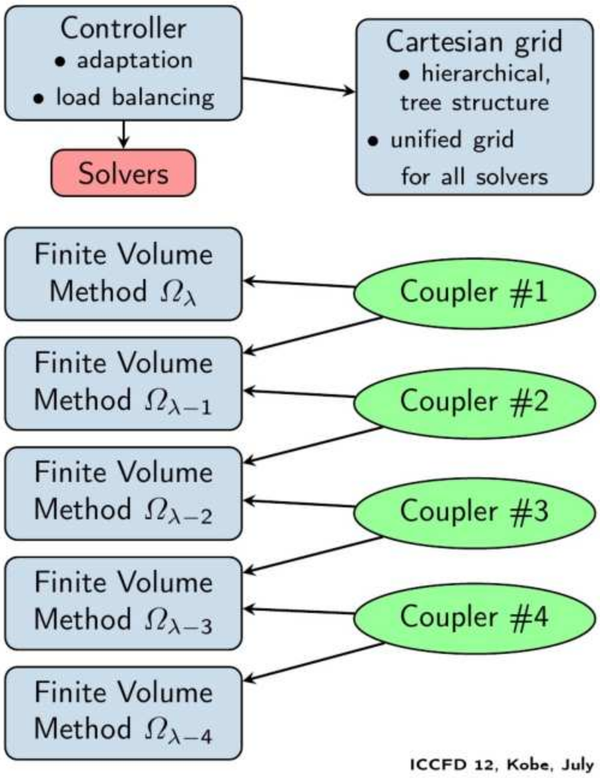

Conservation equations and time integration

Integral form of conservation equations:

$$\frac{d}{dt}\int_{V(t)} \boldsymbol{Q}\, dV = -\oint_{\partial V(t)} \underline{\boldsymbol{H}} \cdot \boldsymbol{n}\, d\Gamma(t) = -\boldsymbol{R}(\boldsymbol{Q})$$

where $V(t) \subset \Omega(t)$ is a moving control volume bounded by the surface $\Gamma(t) = \partial V(t)$ and the outward pointing normal vector $\boldsymbol{n}$. The vector of conserved quantities is defined for the

- Navier-Stokes equations: $\boldsymbol{Q} = [\rho, \rho\boldsymbol{u}, \rho E]^T$
- Heat conduction equation: $\boldsymbol{Q} = H$

Time integration using a second-order accurate ($\alpha_{k-1} = 0.5$) predictor-corrector multistage Runge-Kutta method:

$$(\boldsymbol{Q}V)^{(n,1)} = (\boldsymbol{Q}V)^n - \Delta t\, \boldsymbol{R}^n\left(t^n, \boldsymbol{Q}^n\right)$$

$$(\boldsymbol{Q}V)^{(n,s)} = (\boldsymbol{Q}V)^n - \Delta t \left[\left(1 - \alpha_{s-1}\right) \boldsymbol{R}^n\left(t^n, \boldsymbol{Q}^n\right) + \alpha_{s-1} \boldsymbol{R}^{n+1,s-1}\left(t^{n+1}, \boldsymbol{Q}^{(n,s-1)}\right) \right], \quad s = 2, ..., k$$

$$(\boldsymbol{Q}V)^{n+1} = (\boldsymbol{Q}V)^{(n,k)}$$

Cut-cell formulation

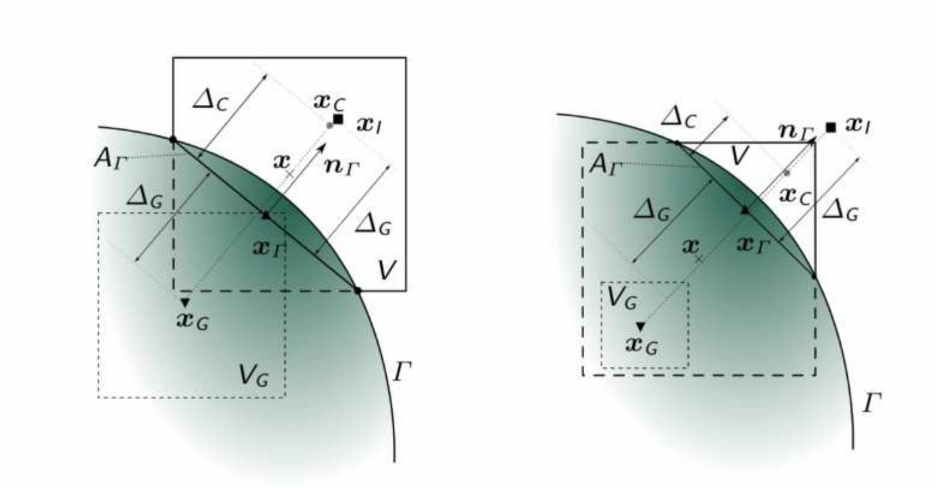

Ghost- ($\boldsymbol{x}_G$) and image point ($\boldsymbol{x}_I$) construction for a single-cut surface Γ in cell C.

$$\boldsymbol{x}_{G,i} = \boldsymbol{x}_C - \max\left(2\Delta_{C,i}, \Delta_{C,i} + \frac{\Delta x}{2}\right) \boldsymbol{n}_{\Gamma,i}\,, \quad \boldsymbol{x}_{I,i} = \boldsymbol{x}_C + \left(\max\left(\Delta_{C,i}, \frac{\Delta x}{2}\right) - \Delta_{C,i}\right) \boldsymbol{n}_{\Gamma,i}$$

Small cells, e.g. $V/\Delta x^d = \omega < 0.5$, pose an upper limit on the time step, since $\Delta t_{\max} = f(\Delta x_{\min})$

Small Cell Correction (Q-SCC) Formulation

Small cell correction based on interpolation of variables and flux redistribution (Q-SCC)

- replace intermediate Runge-Kutta small cell variables $\boldsymbol{Q}_{SC}^{(n,s)}$ by an interpolated value
- interpolation is based on neighbouring cell values NB, and reconstructed surface and ghost cell variables carrying the information of the boundary condition

$$\boldsymbol{Q}_{SC}^{n,s} = \kappa\, \boldsymbol{Q}_{SC,RK}^{n,s} + (1-\kappa) \sum_j^{NB} A_j \boldsymbol{Q}_{j,RK}^{n,s}$$

- Flux redistribution to two neighbouring cell layers, including possibly other small cells, applied in the last Runge-Kutta stage

$$\boldsymbol{Q}_{NB}^{n,k} = \boldsymbol{Q}_{NB,RK}^{n,k} + \sum^{NB} B_{NB}\left(\boldsymbol{Q}_{SC}^{n,k} - \boldsymbol{Q}_{SC,RK}^{n,k}\right).$$

[1] Schneiders et al., *An accurate moving boundary formulation in cut-cell methods*, JCP, 2013
[2] Schneiders et al., *An efficient conservative cut-cell method for rigid bodies interacting with viscous compressible flows*, JCP, 2016
[3] Pember et al., *An adaptive Cartesian grid method for unsteady compressible flow in irregular regions*, JCP, 1995
[4] Colella et al., *A Cartesian grid embedded boundary method for hyperbolic conservation laws*, JCP, 2006

Multigrid Method

- Hierarchical Cartesian mesh with a highest mesh level m offers a simple generation of coarse meshes

$$\Omega_k = \Omega_{k+1} \setminus \{C_{k+1}^n \mid \forall C_{k+1}^n \in \Omega_{k+1}\}\,, \quad k = m-1\ldots 1$$

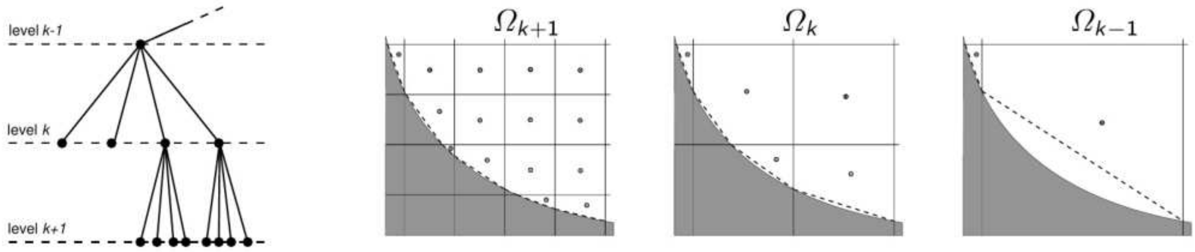

FAS multigrid formulation	$(\boldsymbol{Q}V)_k^{(n,1)} = (\boldsymbol{Q}V)_k^n - \Delta t_k\,(\boldsymbol{R}_k^n(t^n, \boldsymbol{Q}_k^n) + \boldsymbol{\tau}_k^m)$
Defect correction	$\boldsymbol{\tau}_k^m = \overline{I_{k+1}^k}\boldsymbol{\tau}_{k+1}^m + \boldsymbol{R}_k(I_{k+1}^k\boldsymbol{Q}_{k+1}) - \overline{I_{k+1}^k}\boldsymbol{R}_{k+1}(\boldsymbol{Q}_{k+1})$
Injection operator	$I_k^{k-1}(\boldsymbol{Q}_k) = \frac{\sum_\alpha \tilde{\omega}^\alpha V^\alpha \boldsymbol{Q}_k^\alpha}{\sum_\alpha V^\alpha}$
Restriction	$\overline{I_k^{k-1}}(\boldsymbol{R}_k(\boldsymbol{Q}_k)) = \sum_\alpha \omega^\alpha \boldsymbol{R}_k(\boldsymbol{Q}_k^\alpha)$

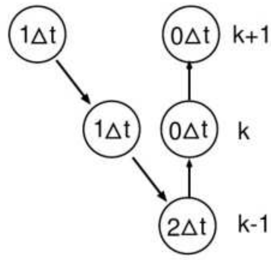

v-cycle

α=number of child cells, ω^α=volume fraction between child and parent cell

Novel Small Cell Correction (R-SCC)

The Q-SCC formulation does not allow a consistent formulation of a defect correction on coarse mesh levels. No convergent solution with a multigrid method could be obtained

Novel R-SCC formulation

- Instead of the variables $\boldsymbol{Q}$ interpolate the flux balance $\boldsymbol{R}$

$$\boldsymbol{R}_{SCI}^{n+1,l} = \kappa\,\boldsymbol{R}_{SC}^{n+1,l} + (1-\kappa)\sum^{NB} A_{NB}\boldsymbol{R}_{NB}^{n+1,l}\frac{V_{SC}}{V_{NB}}$$

- For steady state problems $\boldsymbol{R}$ vanishes such that an conservative solution is obtained without flux redistribution
- For very small cells, convergence to the steady state solution slows down since the boundary condition is only weakly coupled in the R-SCC
- Remedy: use a forcing term for very small cells to drive the cell variable to an interpolated variable taking into account the

$$\boldsymbol{R}_{SCI}^{n+1,l} = \kappa_1\,\boldsymbol{R}_{SC}^{n+1,l} + (1-\kappa_1-\kappa_2)\sum^{NB} A_{NB}\boldsymbol{R}_{NB}^{n+1,l}\frac{V_{SC}}{V_{NB}} + \kappa_2\,F_{SP}\left(\boldsymbol{Q}_{SC}^{n+1,l-1} - \boldsymbol{Q}_{SP}\right),$$

Novel Small Cell Correction (R-SCC)

The Q-SCC formulation does not allow a consistent formulation of a defect correction on coarse mesh levels. No convergent solu

Novel R-SCC formulation

- Instead of the variab

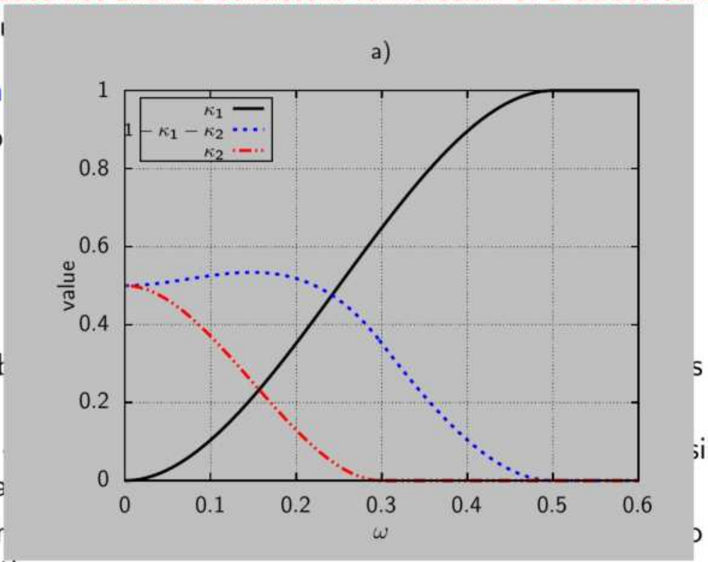

- For steady state prob … s obtained without flux redistribution
- For very small cells, … since the boundary condition is only wea
- Remedy: use a forcir … an interpolated variable taking into account the

$$\boldsymbol{R}_{SCI}^{n+1,l} = \kappa_1\, \boldsymbol{R}_{SC}^{n+1,l} + (1-\kappa_1-\kappa_2)\sum^{NB} A_{NB}\boldsymbol{R}_{NB}^{n+1,l}\frac{V_{SC}}{V_{NB}} + \kappa_2\, F_{SP}\left(\boldsymbol{Q}_{SC}^{n+1,l-1} - \boldsymbol{Q}_{SP}\right),$$

Steady Flow around a Sphere

- Flow around a sphere at Re=100, M=0.1.
- Statically refined mesh, 21.7 million cells, $\Delta x_{min} \approx D/48$
- Domain size $[-24D \ldots 72D, -24D \ldots 24D, -24D \ldots 24D]$

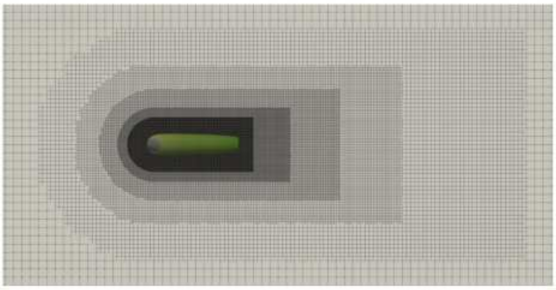

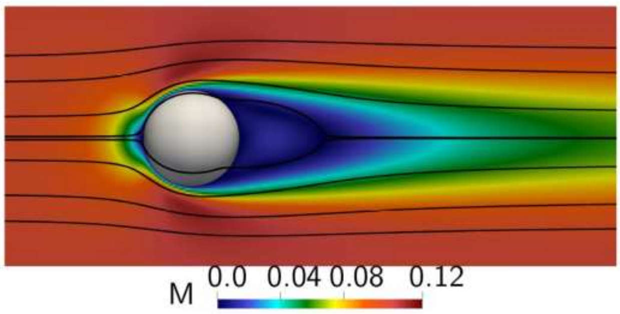

Author	drag coefficient c_D	
Johnson & Patel (JFM 1999)	1.08	boundary fitted mesh
Marella et al.	1.06	cartesian mesh, finite-difference
Hartmann et al.	1.083	cartesian mesh, cell merging
Present Q-SCC	1.087	
Present R-SCC	1.085	

- Flow around a sphere
- Statically refined mes
- Domain size [$-24D$.

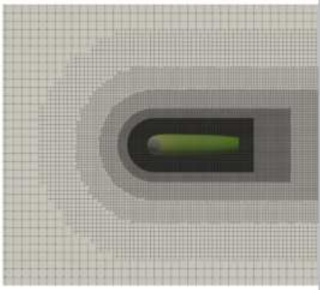

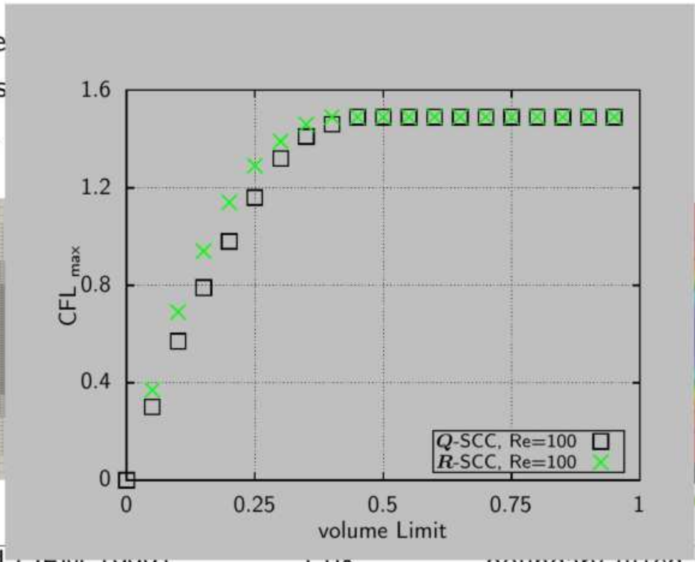

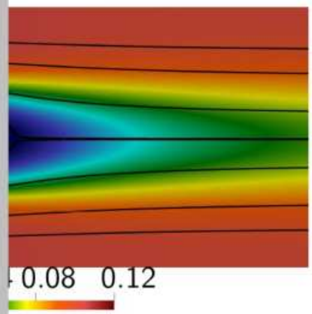

Author		
Johnson & Patel (JFM 1999)	1.08	boundary fitted mesh
Marella et al.	1.06	cartesian mesh, finite-difference
Hartmann et al.	1.083	cartesian mesh, cell merging
Present Q-SCC	1.087	
Present R-SCC	1.085	

- Flow around a sphere at Re=100, M=0.1.
- 3 mesh levels, 21.7, 7.8 & 3.3 million cells
- $\Delta x_{min} \approx D/48$, $\Delta x_{min} \approx D/24$, $\Delta x_{min} \approx D/12$

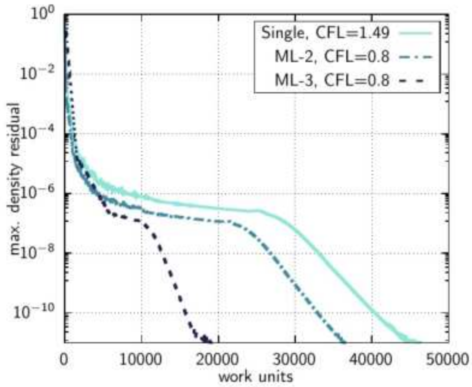

Convergence of the R-SCC method for the flow around a sphere. Results for a single mesh, 2, and with 3 mesh levels and a small cell volume limiter of 0.5

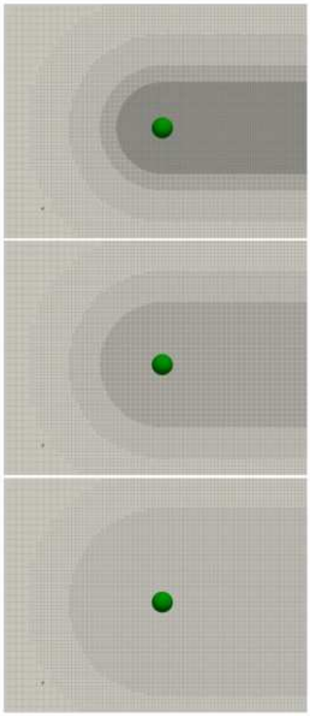

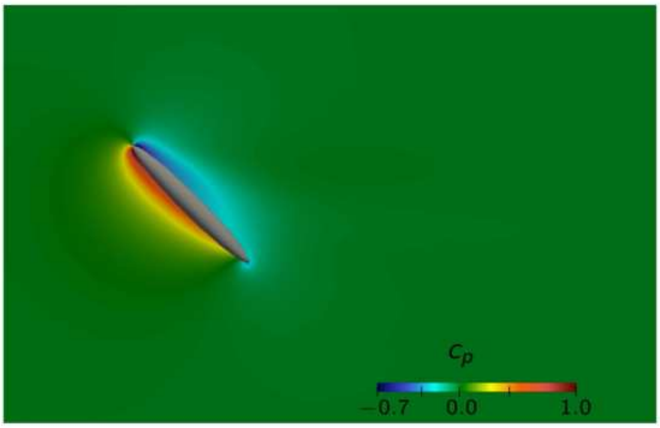

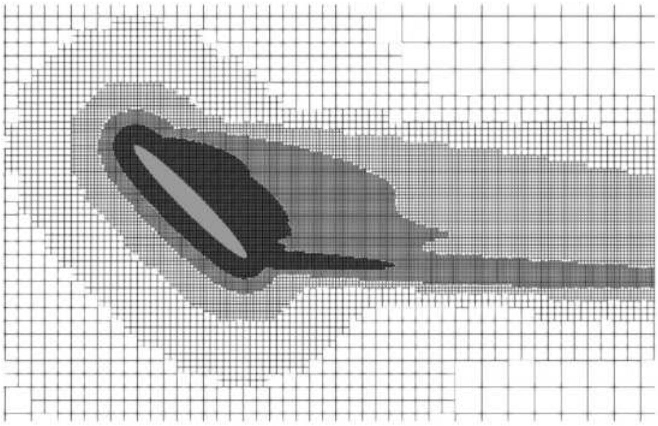

Navier-Stokes solution, pressure coefficient c_p (left), solution adaptive Cartesian mesh (right)

- Re-number Re=100 based on the equivalent diameter D, Mach number M=0.1
- aspect ratio $\beta = 8$, inclination $\varphi = 45°$.
- computational domain size $L_x \times L_y \times L_z = 95D \times 48D \times 48D$, smallest spatial step $\Delta_{\min} = D/48$
- Solution adaptive mesh

Steady Flow around an Ellipsoid

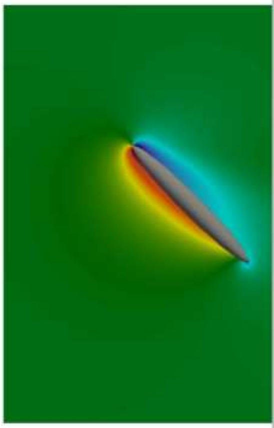

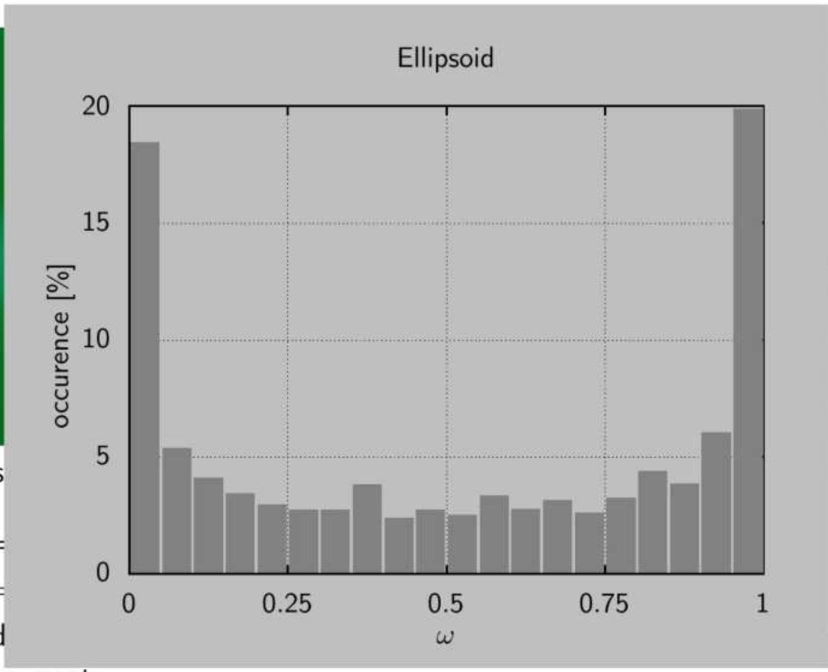

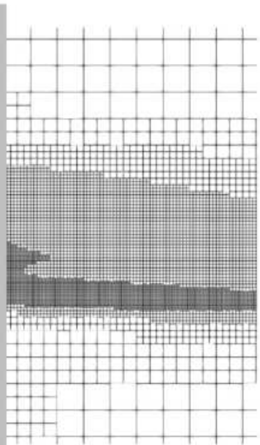

Navier-Stokes s ... mesh (right)

- Re-number Re=
- aspect ratio β =
- computational d ... step $\Delta_{\min} = D/48$
- Solution adaptive mesh

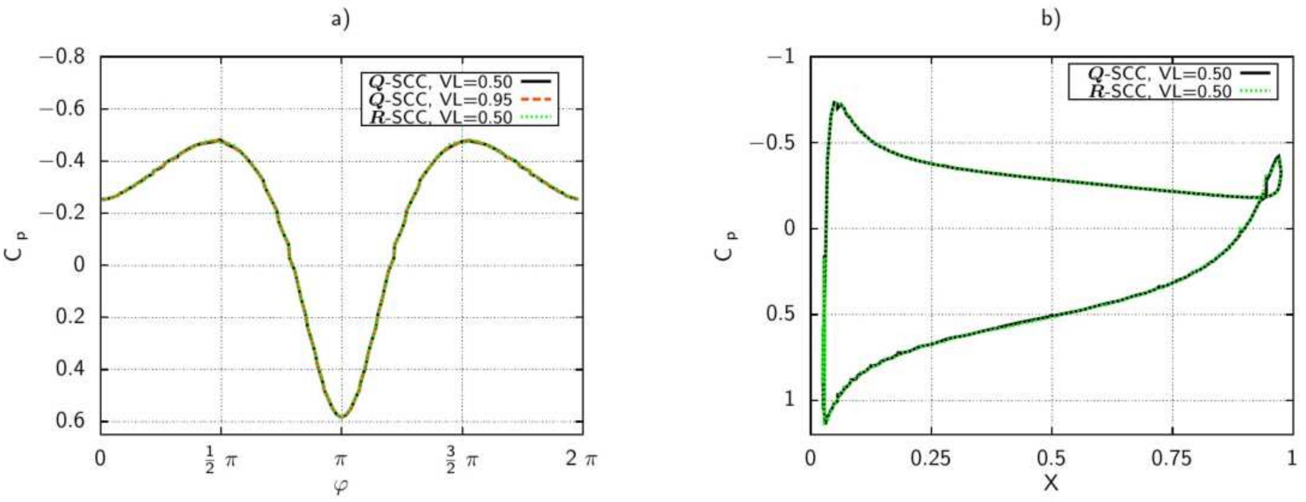

Comparison of results for the Q-SCC and R-SCC formulation for the flow around an ellipsoid

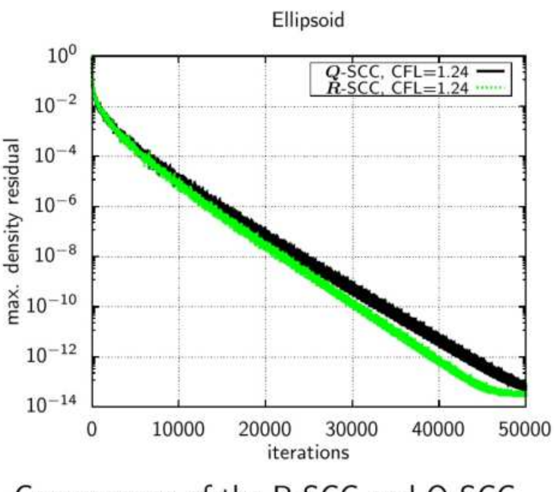

Convergence of the R-SCC and Q-SCC formulation with local time stepping and a small cell limiter $VL = 0.5$

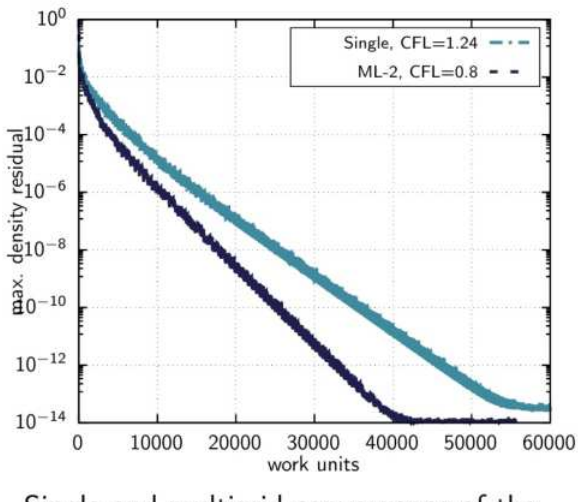

Single and multigrid convergence of the R-SCC formulation with local time stepping and a small cell limiter $VL = 0.5$

Steady Temperature Field in a Slab

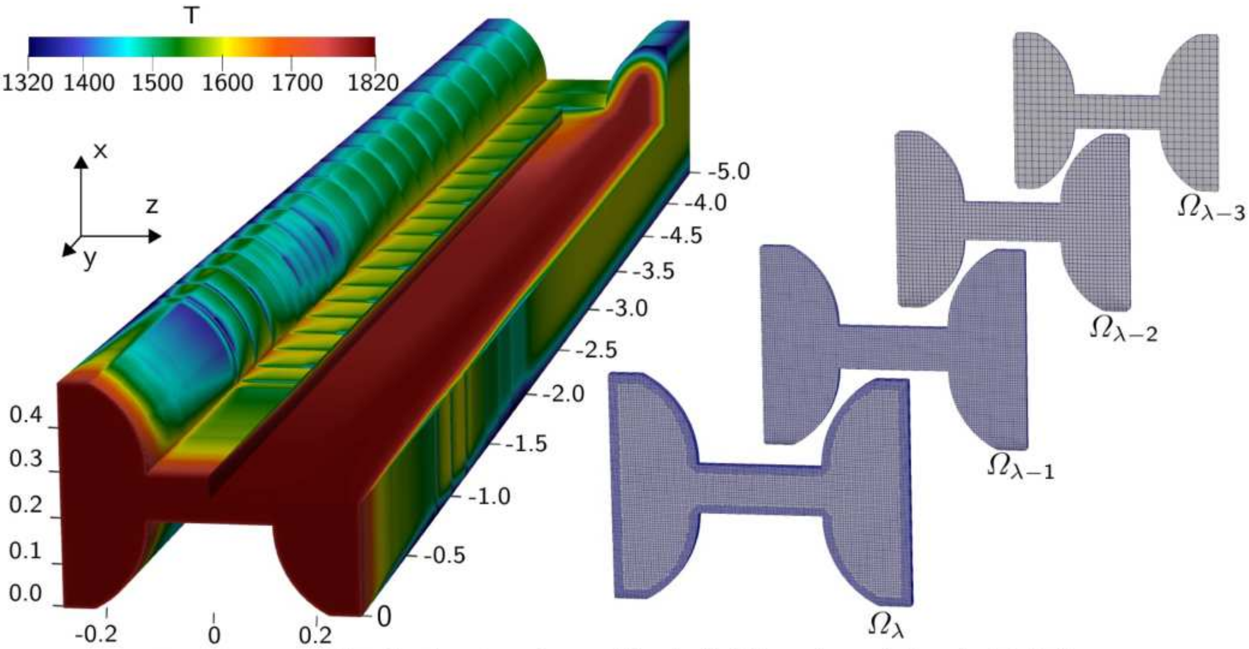

temperature distribution in a beam blank (left) and mesh levels (right)

Steady Temperature Field in a Slab

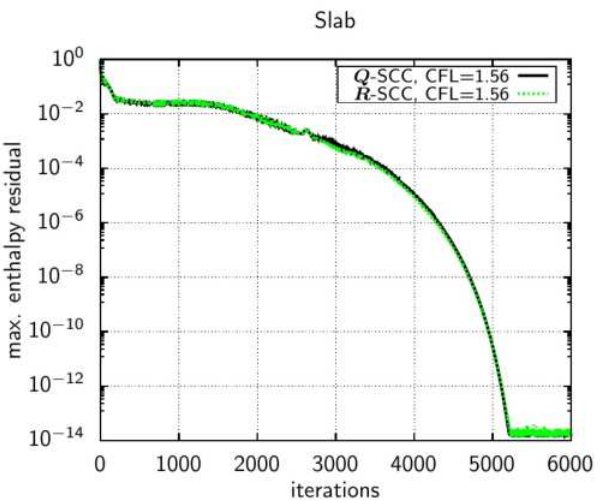

Single grid convergence for the Q-SCC and R-SCC formulation

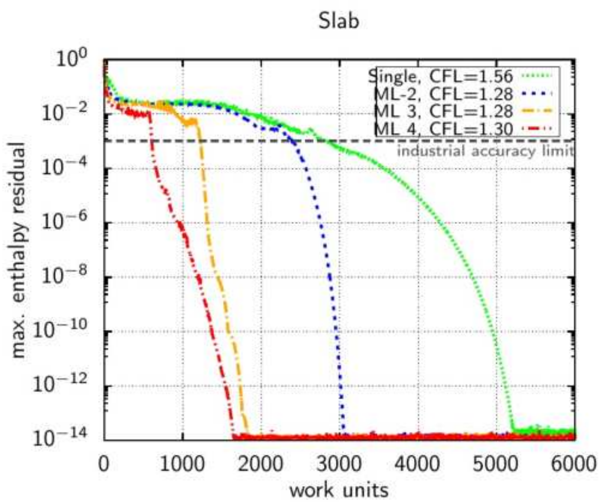

Multigrid convergence for the R-SCC formulation for various numbers of coarse multigrid levels

Summary & Outlook

- Hierarchical Cartesian meshes allow easy implementation of multigrod methods, but small cell corrections formulations may not be suitable
- Interpolation of variables for small cells may not allow to formulate a consistent defect correction and can lead to non-convergent solutions
- Novel small cell corection method has been formulated based on the interpolation of the flux integral
- Acceleration of convergence for the heat conduction by a factor of 10 with four grid levels
- The same small cell correction method is also applicable to CFD applications
- There is optimization potential for the multigrid combined with solution adaptive meshing and in the parallel implementation
- **Future work:** extend the R-SCC to unsteady, moving boundary problems

Summary & Outlook

- Hierarchical Cartesian meshes allow easy implementation of multigrod methods, but small cell corrections formulations may not be suitable
- Interpolation of variables for small cells may not allow to formulate a consistent defect correction and can lead to non-convergent solutions
- Novel small cell corection method has been formulated based on the interpolation of the flux integral
- Acceleration of convergence for the heat conduction by a factor of 10 with four grid levels
- The same small cell correction method is also applicable to CFD applications
- There is optimization potential for the multigrid combined with solution adaptive meshing and in the parallel implementation
- **Future work:** extend the R-SCC to unsteady, moving boundary problems

Thanks for your attention!

Acknowledgements:

SMS group | DFG Deutsche Forschungsgemeinschaft | HLRS